Electronic Supplementary Material (ESI) for Journal of Materials Chemistry A.

Supporting Information

Dopant-Free, Novel Hole Transporting Materials Based on Quinacridone Dye for High-Performance and Humidity Stable Mesoporous Perovskite Solar Cells

Hong Duc Pham,[a]† Sagar M. Jain,[b*]† Li Meng,[b,c] Sergei Manzhos,[e] Krishna Feron,[f,g] Sudhagar Pitchaimuthu,[b] Zhiyong Liu,[h] Nunzio Motta,[a] Hongxia Wang,[a] James R. Durrant,[b,d] Prashant Sonar[a*]

a. Institute of Future Environment and School of Chemistry, Physics and Mechanical Engineering, Queensland University of Technology (QUT), 2 George Street, Brisbane, QLD-4001, Australia.

b. SPECIFIC, College of Engineering, Swansea University Bay Campus, Fabian Way, SA1 8EN Swansea, United Kingdom.

c. Jiangsu Key Laboratory for Carbon-Based Functional Materials and Devices, Institute of Functional Nano and Soft Materials (FUNSOM), Soochow University, Suzhou 215123, China.

d. Department of Chemistry and Centre for Plastic Electronics, Imperial College London, Exhibition Road, London SW7 2AZ, United Kingdom.

e. Department of Mechanical Engineering, Faculty of Engineering, National University of Singapore.

f. CSIRO Energy Centre, NSW-2304, Australia.

g. Centre for Organic Electronics, University of Newcastle, Callaghan, NSW 2308, Australia.

h. Department of Physics and Materials Science, Henan Normal University, Henan Key Laboratory of Photovoltaic Materials, Xinxiang 453007, China

† These authors, H. D. P and S. M. J contributed equally to the work.

Electronic Supplementary Information (ESI) available: [details of any supplementary information available should be included here]. See DOI: 10.1039/x0xx00000x

Email i.d. of corresponding authors

sonar.prashant@qut.edu.au and sagarmjain@gmail.com or s.m.jain@swansea.ac.uk

Experimental Details:

Materials and Instruments:

All chemicals and reagents were purchased from commercial vendors and used directly without any further purification. Reactions were monitored by thin layer chromatography (TLC) and were carried out under argon atmosphere.

^{1}H and ^{13}C NMR spectra were performed on a Bruker 600 MHz spectrometer. High-resolution mass spectra were acquired on an LTQ Orbitrap Elite mass spectrometer (Thermo Fisher Scientific, Bremen, Germany) equipped with an electrospray ionisation (ESI) source, operating in the positive ion mode at a resolution of 120,000 (at *m/z* 400). Reserpine ($[M+H]^+$, *m/z* 609.28066) was used as a lockmass calibrant to increase the measurement accuracy. UV-Vis spectra were recorded on a Shimadzu UV-1800 spectrometer. Differential-scanning-calorimetry (DSC) was performed using a Q100 DSC Chimaera equipped with a cooling apparatus. The thermogravimetric analysis (TGA) was performed using a Q500TGA Pegasus. Photoelectron spectroscopy in air (PESA) measurements was conducted using on an AC-2 photoelectron spectrometer (Riken-Keiki Co.).

Synthesis

2,9-bis(1,2-dihydroacenaphthylen-5-yl)-5,12-dioctyl-5,12-dihydroquinolino[2,3-*b*]acridine-7,14-dione (**ACE-QA-ACE**):

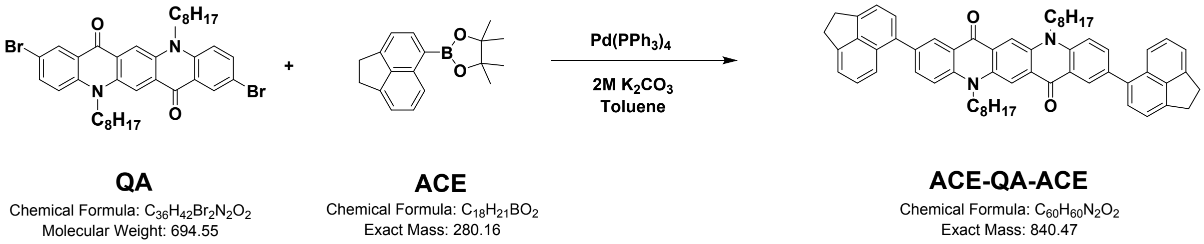

In a three-neck round bottom flask, 2,9-dibromo-5,12-dioctyl-5,12-dihydroquinolino[2,3-*b*]acridine-7,14-dione (**QA**) (200 mg, 0.288 mmol) and 2-(1,2-dihydroacenaphthylen-5-yl)-4,4,5,5-tetramethyl-1,3,2-dioxaborolane (ACE) (218mg, 0.777 mmol) and 2M aqueous K_2CO_3 solution (12 mL) were dissolved in degassed toluene (19 mL). The solution was purged with argon for 15 minutes, then tetrakis(triphenylphosphine)palladium (16.18 mg 0.014 mmol) was added. The reaction was stirred at 120 °C for 2 days. After the reaction mixture was cooled to room temperature and extracted with chloroform and water. The organic layer was dried over anhydrous Na_2SO_4 and concentrated by evaporation. The solvent was evaporated and the crude product recrystallized from hot acetone to afford the desire compound as a pink solid (150 mg, 62%). ^{1}H NMR (600 MHz, $CDCl_3$, ppm): δ 8.81-8.76 (m, 4H), 7.96 (dd, J_1 = 8.8 Hz, J_2 = 1.8 Hz, 2H), 7.72 (d, J = 8.4 Hz, 2H), 7.60 (d, J = 8.9 Hz, 2H), 7.48 (d, J = 7.0 Hz, 2H), 7.39 (m, 2H), 7.33 (d, J = 7.0 Hz, 2H), 7.28 (d, J = 4.4 Hz, 2H), 4.54 (m, 4H), 3.41 (m, 8H), 2.03 (m, 4H), 1.60 (m, 4H), 1.43 (m, 4H), 1.32 (m, 4H), 1.25 (m, 8H), 0.83 (m, 6H). ^{13}C NMR (150 MHz, $CDCl_3$, ppm): δ 178.26, 146.36, 145.94, 141.44, 139.69, 136.42, 135.81, 134.12, 133.16, 129.37, 128.92, 128.50, 128.32, 126.48, 121.30, 120.57, 119.54, 119.29, 114.78, 113.68, 46.59, 31.82, 30.60, 30.09, 29.46, 29.35, 27.31, 27.12, 22.67, 14.12. ESI-MS: $C_{60}H_{60}N_2O_2^{+\bullet}$ *m/z* 841.58 (calculated *m/z* 840.47)

2,9-bis(4-(bis(4-methoxyphenyl)amino)phenyl)-5,12-dioctyl-5,12-dihydroquinolino[2,3-*b*]acridine-7,14-dione (**TPA-QA-TPA**):

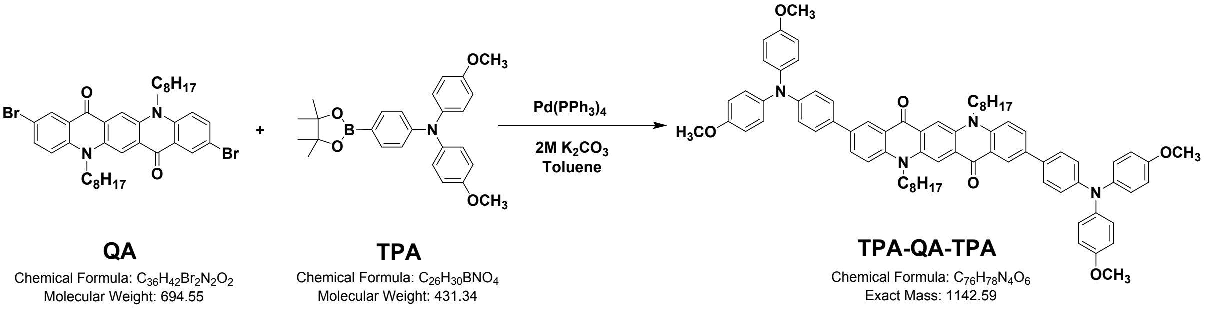

In a three-neck round bottom flask, QA (200 mg, 0.288 mmol), 4-methoxy-*N*-(4-methoxyphenyl)-*N*-(4-(4,4,5,5-tetramethyl-1,3,2-dioxaborolan-2-yl)phenyl)aniline (TPA) (340 mg, 0.778 mmol), and 2M aqueous K_2CO_3 solution (12 mL) were dissolved in degassed toluene (19 mL). The solution was purged with argon for 15 minutes, then tetrakis(triphenylphosphine)palladium (16.18 mg 0.014 mmol) was added. The reaction was stirred at 120 °C for 2 days. After the reaction mixture was cooled to room temperature and extracted with chloroform and water. The organic layer was dried over anhydrous Na_2SO_4 and concentrated by evaporation. The solvent was evaporated and the crude product recrystallized from hot acetone to afford the desire compound as a red solid (180 mg, 54.7%). ^1H NMR (600 MHz, $CDCl_3$, ppm): δ 8.61-8.55 (m, 4H), 7.79 (m, 2H), 7.37 (m, 6H), 6.95 (d, *J* = 8.9 Hz, 8H), 6.87 (d, *J* = 6.8 Hz, 4H), 6.70 (d, *J* = 8.8 Hz, 8H), 4.36 (m, 4H), 3.65 (s, 12H), 1.84 (m, 4H), 1.46 (m, 4H), 1.30 (m, 4H), 1.20 (m, 4H), 1.14 (m, 8H), 0.73 (t, *J* = 6.8 Hz, 6H). ^{13}C NMR (150 MHz, $CDCl_3$, ppm): δ 178.01, 155.95, 141.65, 135.99, 132.59, 127.02, 126.83, 126.68, 125.85, 124.35, 121.27, 120.86, 115.98, 114.87, 114.80, 114.71, 114.37, 55.52, 49.68, 38.36, 30.96, 28.77, 24.37, 23.06, 13.99, 11.22. ESI-MS: $C_{76}H_{78}N_4O_6^{+\bullet}$ *m/z* 1143.21 (calculated *m/z* 1142.59)

2,9-bis(bis(4-methoxyphenyl)amino)-5,12-dioctyl-5,12-dihydroquinolino[2,3-*b*]acridine-7,14-dione **(DPA-QA-DPA)**:

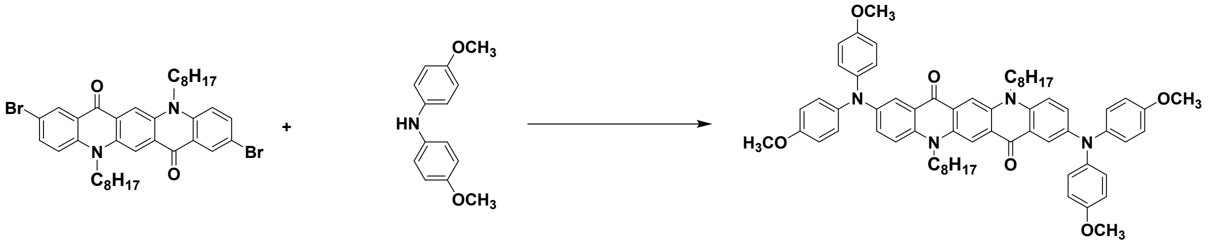

QA
Chemical Formula: $C_{36}H_{42}Br_2N_2O_2$
Molecular Weight: 694.55

DPA
Chemical Formula: $C_{14}H_{15}NO_2$
Molecular Weight: 229.28

DPA-QA-DPA
Chemical Formula: $C_{64}H_{70}N_4O_6$
Exact Mass: 990.53

In a three-neck round bottom flask, QA (200 mg, 0.288 mmol), bis(4-methoxyphenyl)amine (180 mg, 0.778 mmol) and NaO^tBu (70 mg, 0.72 mmol) were added and vacuumed for 30 min. Afterwards, anhydrous toluene (25 ml) and $^tBu_3P$ (1M toluene solution, 20μl, 0.02 mmol) were added to dissolve the solid and degassed by argon for 30 min. Then, $Pd_2(dba)_3$ (22.2mg, 0.024mmol) was added and the mixture was vacuumed and degassed for 30 min. Subsequently, the reaction was stirred at 110 °C for 2 days. After the reaction mixture was cooled to room temperature and extracted with chloroform and water. The organic layer was dried over anhydrous Na_2SO_4 and the solvent removed under reduced pressure. The residue was purified using silica gel column chromatography with a mixture of hexane and chloroform as eluent. Then the crude product recrystallized from hot methanol to yield the desired compound as dark green solids (110 mg, 39%). ^1H NMR (600 MHz, $CDCl_3$): δ 8.73 (s, 2H), 8.12 (s, 2H), 7.54-7.52 (d, *J* = 7.2 Hz, 2H), 7.43-7.41 (d, *J* = 9.6 Hz, 2H), 7.09 (s, 8H), 6.87-6.86 (d, *J* = 8.4 Hz, 8H), 4.48 (s, 4H), 3.83 (s, 12H), 2.03-1.98 (m, 4H), 1.62-1.57 (m, 4H), 1.47-1.42 (m, 4H), 1.38-1.29 (m, 12H). ^{13}C NMR (120 MHz, $CDCl_3$): δ 177.46, 155.80, 142.74, 140.98, 137.44, 135.19, 129.99, 125.96, 125.64, 121.88, 117.71, 115.60, 114.88, 113.20, 55.54, 46.50, 31.78, 29.32, 27.07, 22.64, 14.10. ESI-MS: $C_{64}H_{70}N_4O_6^{+\bullet}$ *m/z* 991.67 (calculated *m/z* 990.53)

Substrates Preparation:

A patterned FTO-coated glass (13 Ω sq -1 , Aldrich) was etched by Zn powder and 2 M HCl diluted in deionized water. Subsequently, the substrates were cleaned with detergent diluted in deionized water, rinsed with deionized water, acetone and ethanol, and dried with clean dry air. A compact blocking layer of TiO_2 (40 nm, c-TiO_2) was deposited on the fluorine doped SnO_2 (FTO, Pilkington, TEC8) substrate by spray pyrolysis using a 20 mM titanium di-isopropoxide bis(acetylacetonate) solution (Aldrich) at 500oC for 30 minutes.[1] To deposit the mesoporous TiO_2 layer, Dyesol DSL 30 NR-D paste is dissolved in anhydrous isopropanol and kept for sonication for 1 hours. Once the solution is homogeneous it is ready to deposit on FTO/Compact TiO_2 substrate by spin coating at 3000 rpm for 30 second followed by annealing at 550 ^{o}C estimated to give ~400 nm thick layer.[2]

Fabrication of Devices:

The PSCs were prepared by one step spin coating of a $CH_3NH_3PbI_3$ solution. The solution was prepared in DMF/DMSO = 6:4 by mixing CH_3NH_3I (0.199 gm) and PbI_2 (0.600 gm). The solution was heated at 60 ^{o}C for 3 hours for mixing. Then the solution was spin coated using Chlorobenzene as antisolvent at rpm of 4000 for 30 s, and annealed for 30 minutes at 100 ^{o}C on a hotplate. The absorber perovskite material with electrode (FTO/Compact-TiO_2/Mesoporous TiO_2) is ready after the above annealing procedure. The electrodes with the absorber material were allowed to cool down to room temperature. A solution containing Spiro-OMe-TAD in chlorobenzene and additives (10 μl ml^{-1} *t*-BP, 32 μl ml^{-1} Li-TFSI solution: 600 Mm in acetonitrile) was spin coated onto the perovskite film at 5000 rpm, for 30 second. Finally, 80 nm thick silver contacts were evaporated at 10^{-4} torr. Similarly, other hole transporting materials, ACE-QA-ACE, TPA-QA-TPA and DPA-QA-DPA were dissolved in 40 mg in 1 ml chlorobenzene and kept for sonication for 30 minutes. The solution was filtered (0.45 ɰ) before use and spin coated on top of perovskite absorber at 5000 rpm for 30 seconds followed by annealing at 550 ^{o}C estimated to give ~400 nm thick layer.[2]

Power Conversion Efficiency and Incident Photon to Current Conversion Efficiency (IPCE): Masked devices (0.100 cm^{2}) were tested under a class AAA solar simulator (Newport Oriel Sol3A) at AM1.5 and 100 mW cm^{-2} illumination conditions calibrated against a KG5 filtered silicon reference cell (Newport Oriel 91150-KG5) using a Keithley

2400 source meter. Current–voltage sweeps were performed from forward-to-reverse bias at a rate of 0.1V s^{-1}.

Stability Measurements - Humidity Test:

Stability tests on optimized champion devices without encapsulation for different hole transporting material were performed. The solar cells were kept in relative humidity of 75% at room temperature in the dark. Continuous 1 sun illumination: The non-encapsulated cells are placed in a cell holder with a glass cover and are in direct contact with ambient atmosphere. For the stability the cells are kept at 35oC temperature, under 1sun illumination using solar simulator class A 1.5 M at full sun under short circuit condition for 200 hours. IV curves were characterized by an electronic system using 22 bits delta-sigma analogic to digital converter. For IV curves measurement, a scan rate of 10 mV s^{-1} with a step of 5 mV was used, maintaining the temperature of the holder to 35 ^{o}C while the temperature of the cells was measured around 45 ^{o}C. The systemcomprises a set of I–V curves at different light intensities (dark current, 10 and 100 mW cm^{-2}). Between each measurement the cells are maintained at the maximum power point using a MPPT algorithm under 100 mW cm^{-2}.

Hole Transport Measurements:

Space charge limited current (SCLC) method PEDOT: PSS (Poly(3,4-ethylendioxythiophene)–poly (styrene sulfonate)) was spin-coated onto indium tin oxide substrate (ITO) and dried at 130 ºC for 20 minutes in vacuum. The purpose of PEDOT: PSS layer (40 nm) was to reduce the roughness of ITO as well as to improve the work function, achieving enhanced hole-only device properties. The HTMs were spincoated onto PEDOT: PSS from chloroform solution (30 mg/mL) in a nitrogen atmosphere. Finally, Au contacts (400 nm thick) were applied via thermal evaporation through a shadow mask in 2×10^{-6} Torr vacuum. The work function of Au and ITO are close to the HOMO energy level of the HTM as well as far below the LUMO energy level. Therefore, the electron injection barrier is higher than the corresponding hole injection barrier. As a result, the transport is dominated by holes. The J–V characteristics of the sample was measured with a Keithley 2420 source meter unit at room temperature. The device configuration and equations to extract mobility has been reported by us previously.[3]

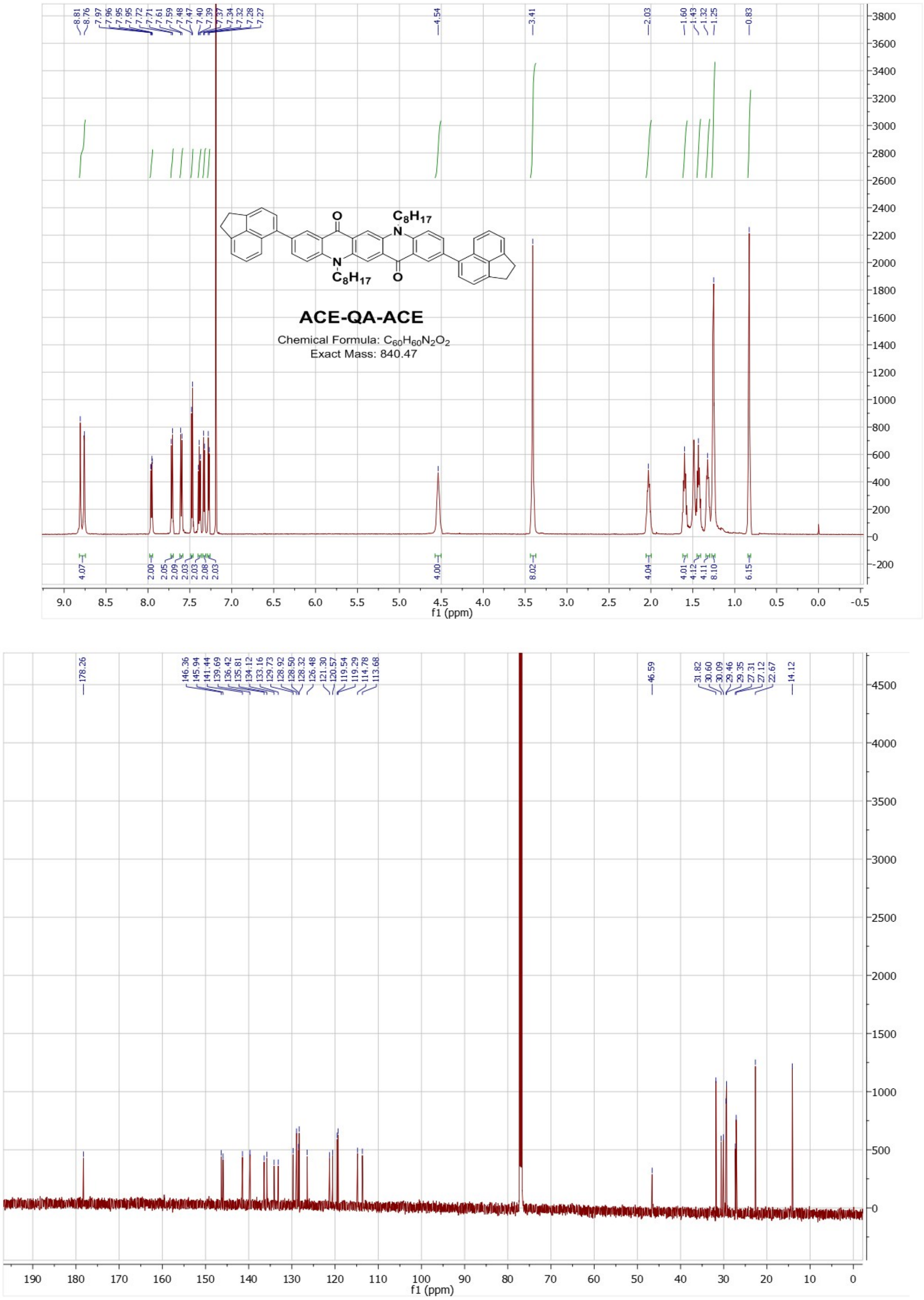

Fig. S1. (a) ^{1}H (600 MHz, CDCl$_3$) spectrum and (b) ^{13}C NMR (120 MHz, CDCl$_3$) spectrum of (**ACE-QA-ACE**).

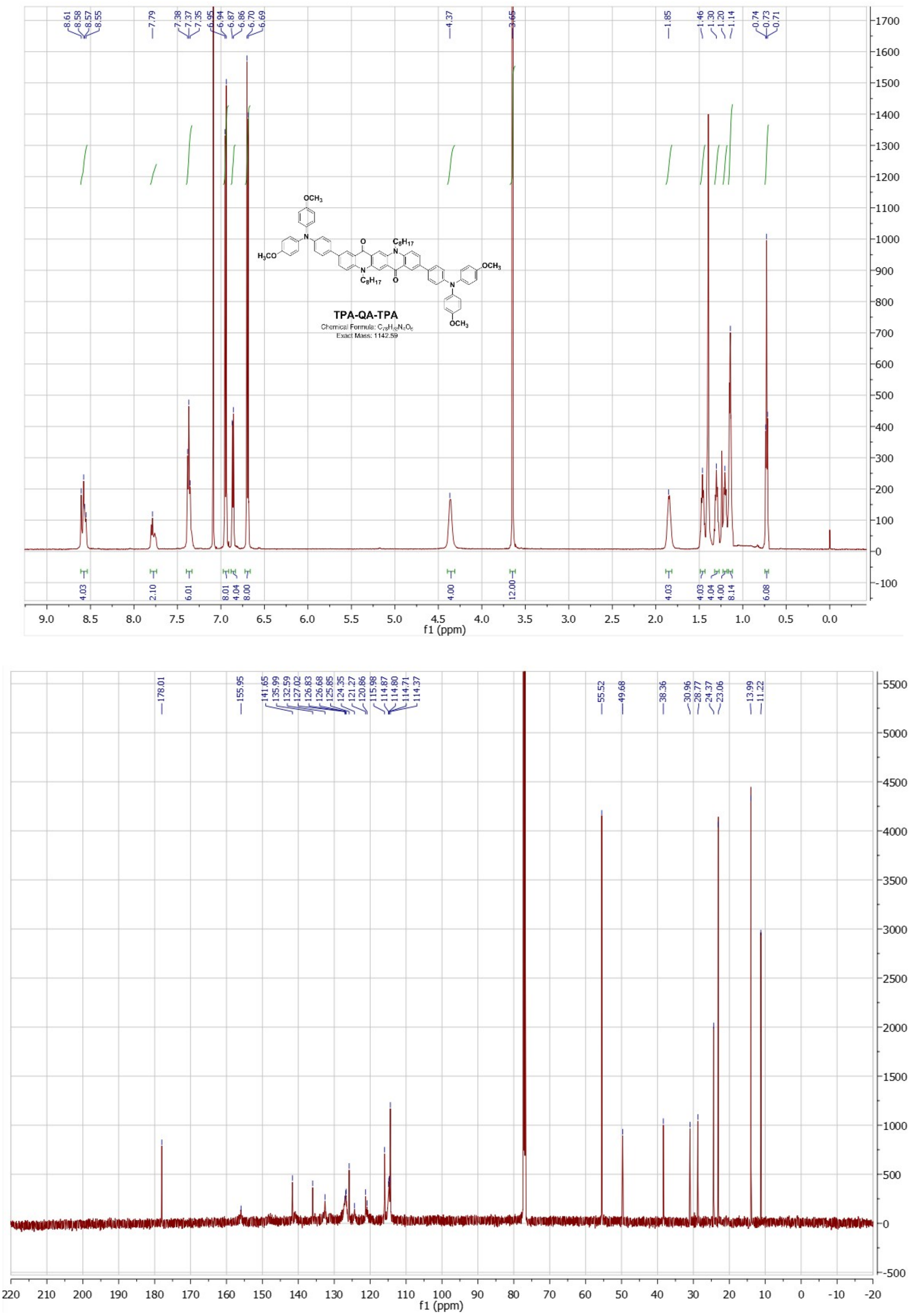

Fig. S2. (a) ^{1}H (600 MHz, $CDCl_3$) spectrum and (b) ^{13}C NMR (120 MHz, $CDCl_3$) spectrum of (**TPA-QA-TPA**).

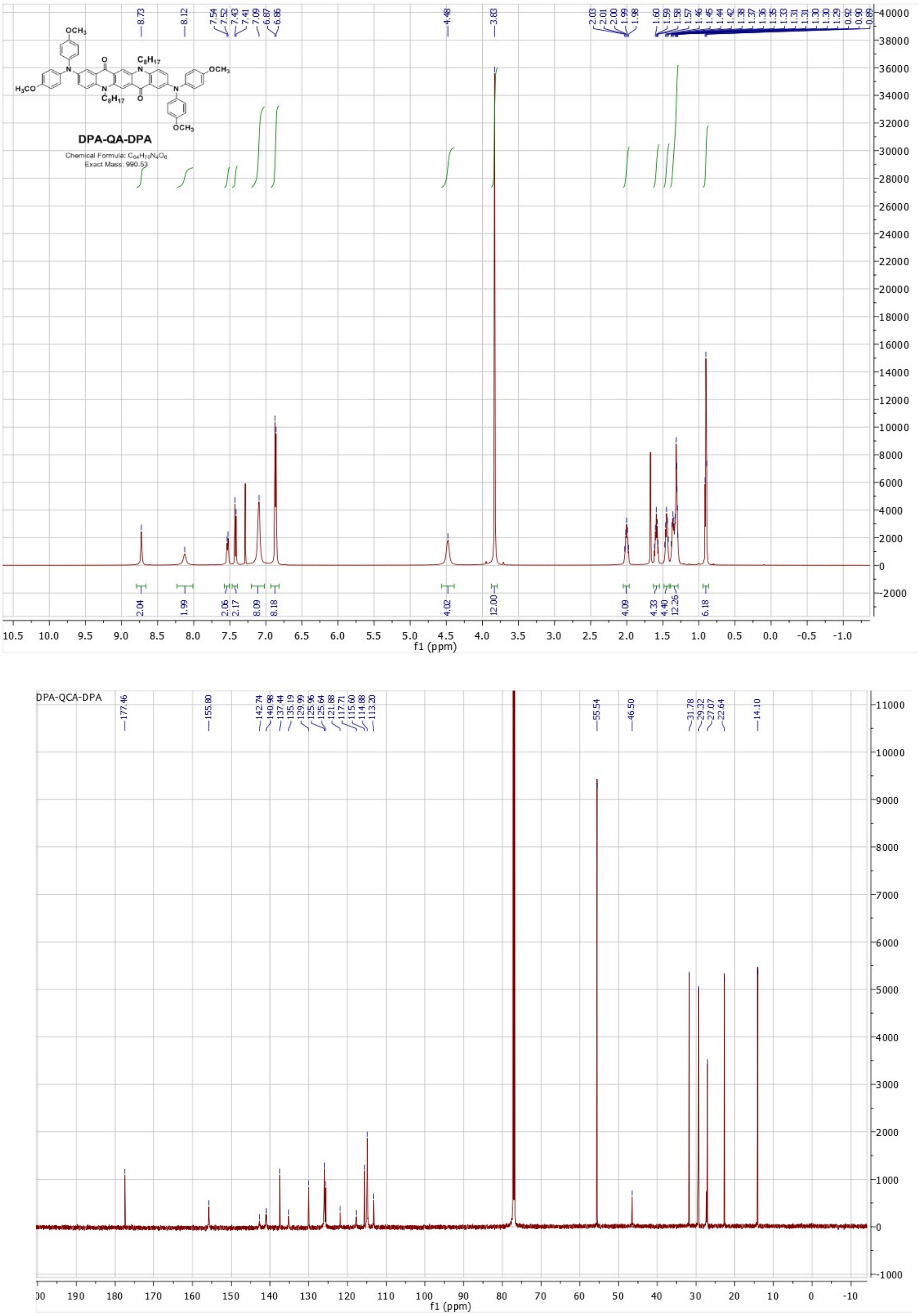

Fig. S3. (a) ^{1}H (600 MHz, $CDCl_3$) spectrum and (b) ^{13}C NMR (120 MHz, $CDCl_3$) spectrum of (**DPA-QA-DPA**).

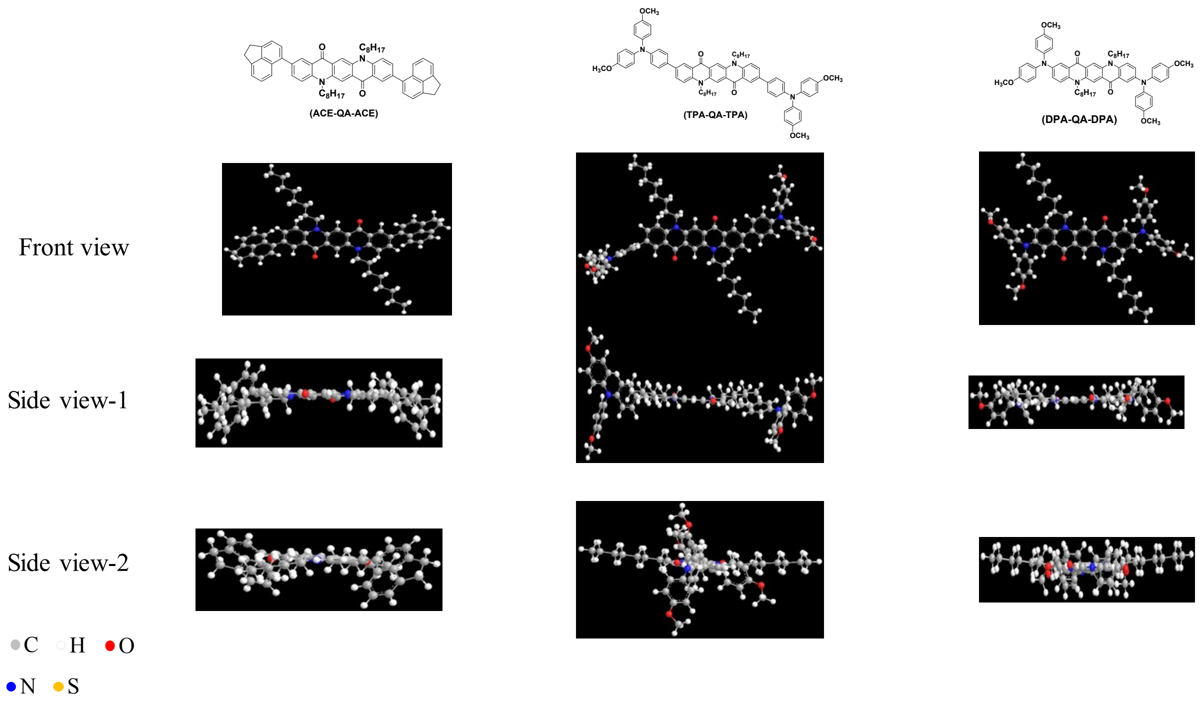

Fig. S4. Chemical structure and front-side views of three new semiconductors.

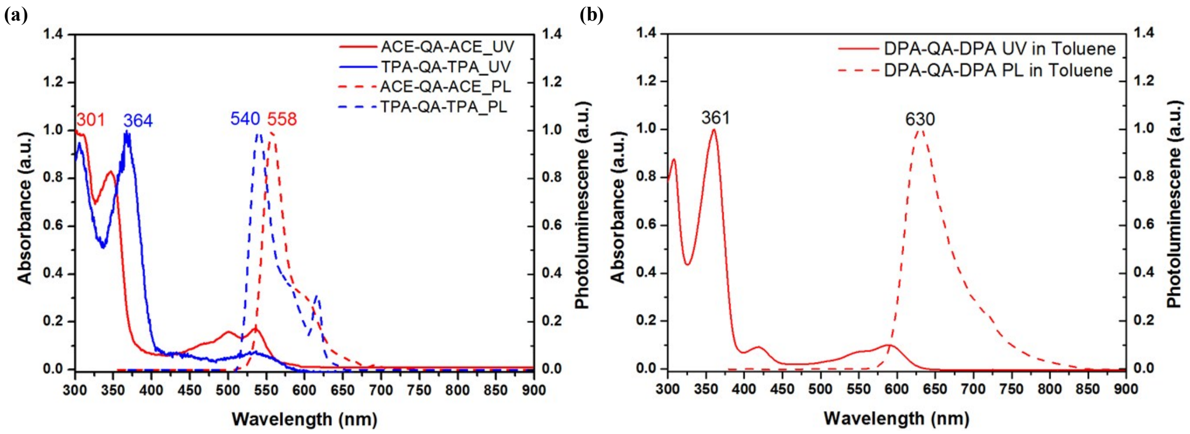

Fig. S5. (a) Normalised absorption and emission spectra of ACE-QA-ACE and TPA-QA-TPA in CF solution; (b) Normalised absorption and emission spectra of DPA-QA-DPA in Toluene solution.

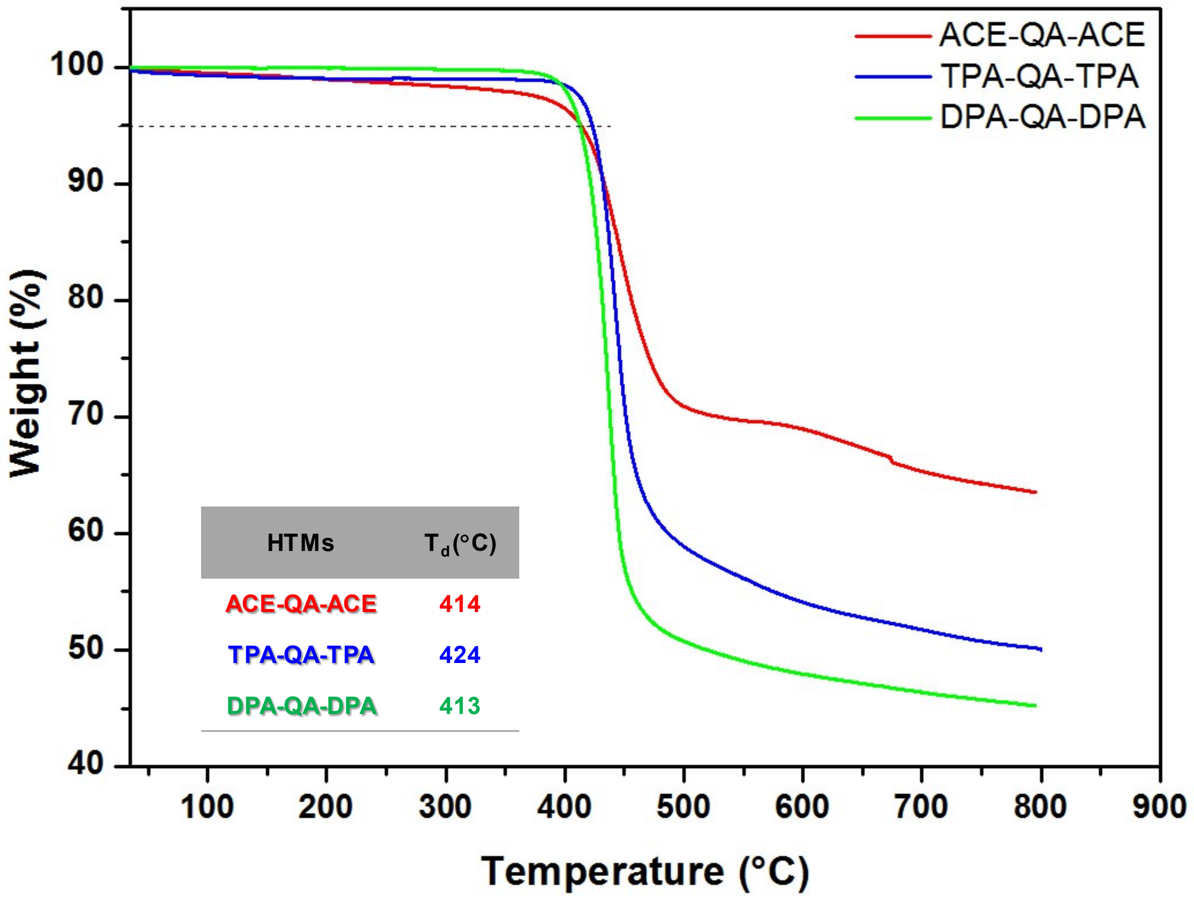

HTMs	T_d(°C)
ACE-QA-ACE	414
TPA-QA-TPA	424
DPA-QA-DPA	413

Fig. S6 Thermogravimetric analysis (TGA) curve of three new materials.

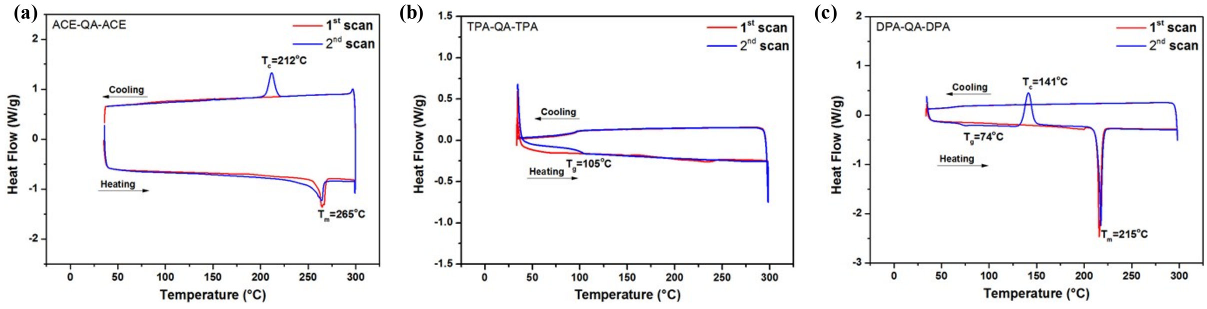

Fig. S7 Differential scanning calorimetry (DSC) of (a) ACE-QA-ACE, (b) TPA-QA-TPA and (c) DPA-QA-DPA with scan rate of 10 °C/min under N_2 atmosphere.

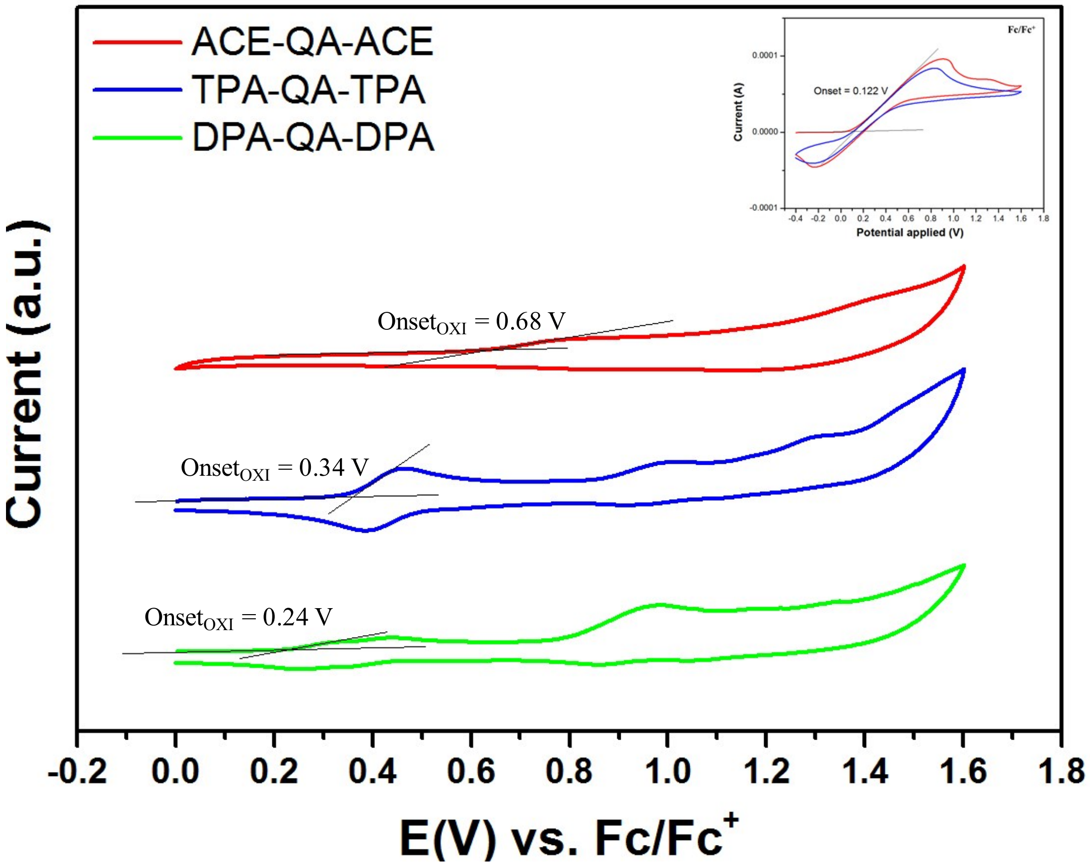

Fig. S8 Cyclic voltammograms of three new compounds. The oxidation was measured in DCM/0.1M Bu_4NPF_6 at a scan rate of 100 mV/s.

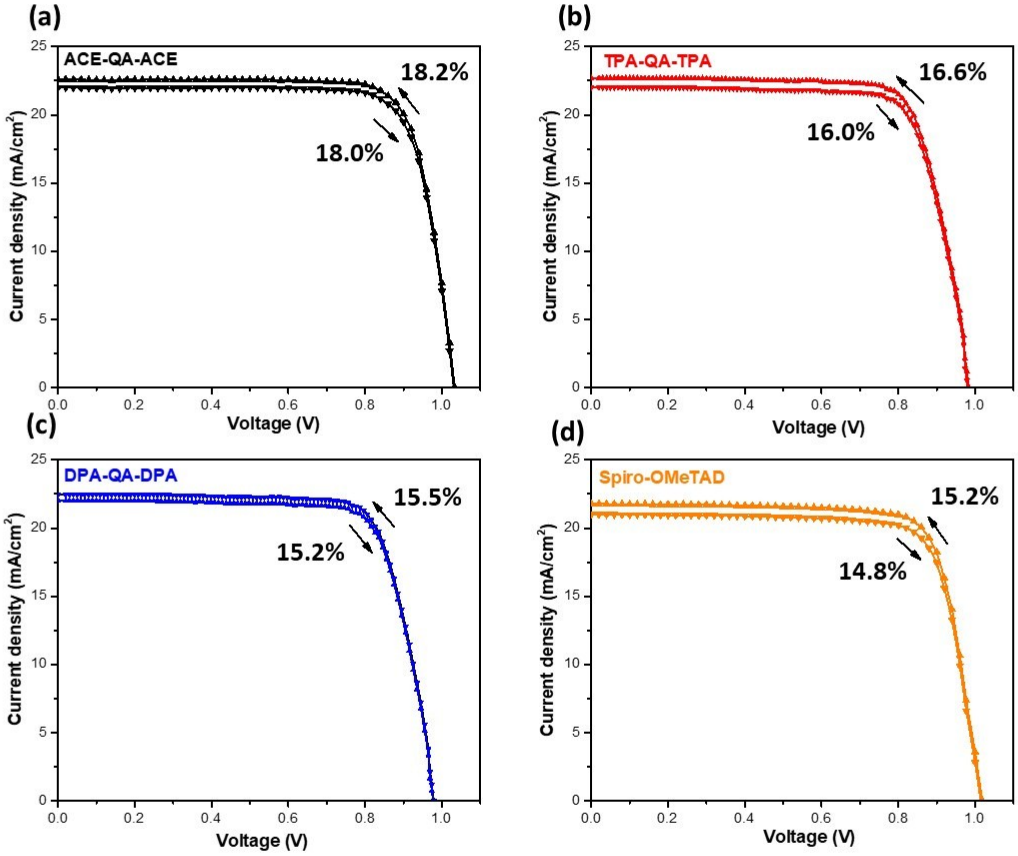

Fig. S9 Hysteresis behaviour of champion solar cells made using ACE-QA-ACE (black curve) , TPA-QA-TPA (red curve), DPA-QA-DPA (blue curve) and Spiro-OMeTAD (orange curve) as HTLs. Scan from 0 V to Voc at a constant scan speed of 0.1 mV/s.

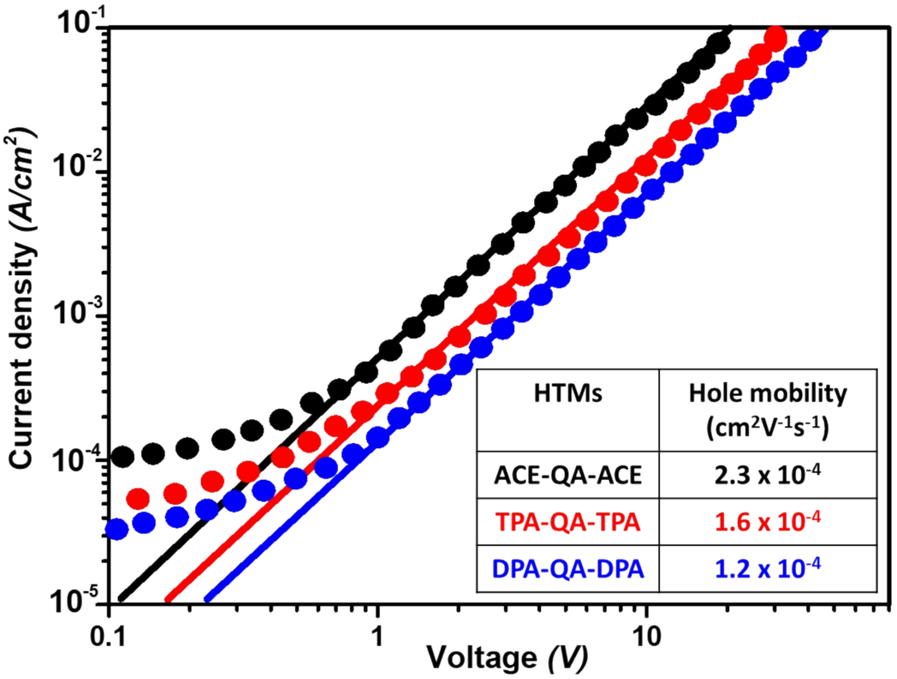

HTMs	Hole mobility ($cm^2V^{-1}s^{-1}$)
ACE-QA-ACE	2.3×10^{-4}
TPA-QA-TPA	1.6×10^{-4}
DPA-QA-DPA	1.2×10^{-4}

Fig. S10 J-V data for space charge limited current (SCLC) method of hole-mobility determination.

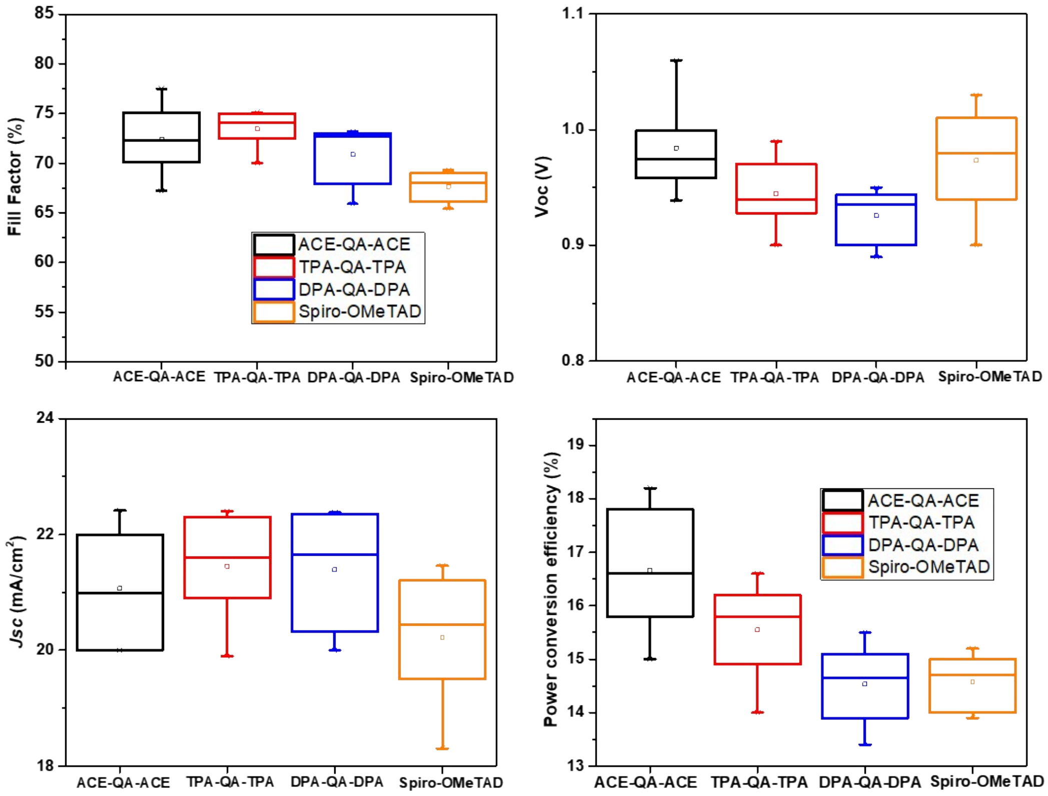

Fig. S11 Statistics of the photovoltaic parameters of 40 perovskite devices fabricated employing Spiro-OMeTAD and respective QA derivative HTMs.

Table S1. Density Functional Theory (DFT) and Time-Dependent DFT (TD-DFT) calculations of ACE-QA-ACE, TPA-QA-TPA and DPA-QA-DPA.

Compound	ACE-QA-ACE	TPA-QA-TPA	DPA-QA-DPA
HOMO, eV	-5.34	-4.93	-4.85
LUMO, eV	-2.64	-2.63	-2.59
gap, eV	2.69	2.31	2.26
VIS peak(s), nm	529.44	616.67	655.63
osc strength	0.0717	0.0556	0.0673
composition	H->L	H->L	H->L
dihedrals TPA-core	47.3	27.7	n/a

Table S2. The comparison of small molecular organic dyes derivatives based HTMs[a)]

Organic dye	HTM	Additives	HOMO [eV]	Hole mobility [$10^{-4}cm^{2}V^{-1}s^{-1}$]	Active area [cm^{2}]	V_{oc} [V]	J_{sc} [$mAcm^{-2}$]	FF [%]	PCE [%][b)]	Ref.
Quinacridone	TPA-QA-TPA	None	-5.41	1.6	0.1	0.99	22.4	75.1	16.6 (15.2)[c)]	This study
	ACE-QA-ACE	None	-5.59	2.3	0.1	1.06	22.41	77	18.2 (15.2)	
	DPA-QA-DPA	None	-5.28	1.2	0.1	0.95	22.38	73.2	15.5 (15.2)	
Anthanthrone	TPA-ANT-TPA	None	-5.41	2.6	0.1	1.03	21.07	79.6	17.5 (16.8)[f)]	4
	ACE-ANT-ACE	None	-5.14	0.24	0.1	1.03	18.7	67.1	13.1 (16.8)	4
	DPA-ANT-DPA	None	-5.46	1	0.1	1.00	16.2	71	11.5 (16.0)	5
Carbazole	CZ-TA	Li-TFSI	-5.11	1.65	0.08	1.044	21.66	81	18.32 (18.28)	6
	B186	Li-TFSI *t*-BP	-4.53	-	0.24	0.98	20.11	73.27	14.59 (17.68)	7
	B74	Li-TFSI *t*-BP	-4.67	-	0.24	0.94	14.75	93.71	11.51 (17.68)	7
	3,6 BCz-OMeTAD	None	-5.11	1.13	0.1	1.121	21.34	71.4	17.0 (18.5)	8
	2,7 BCz-OMeTAD	None	-5.15	0.95	0.1	1.089	22.38	72.5	17.6 (18.5)	8

[a)] The photovoltaic parameters of the solar cells with HTMs evaluated under 1 sunlight illumination (100 mW cm^{-2}) condition.

[b)] The best PCE of the HTMs based devices.

[c)] The best PCE of the standard doped SPIRO-OMeTAD.

References:

1. S. M. Jain, Z. Qiu, L. Häggman, M. Mirmohades, M. B. Johansson, T. Edvinsson and G. Boschloo, *Energy Environ. Sci.*, 2016, **9**, 3770-3782.
2. S. M. Jain, B. Philippe, E. M. J. Johansson, B.-w. Park, H. Rensmo, T. Edvinsson and G. Boschloo, *J. Mater. Chem. A*, 2016, **4**, 2630-2642.
3. M. Planells, A. Abate, D. J. Hollman, S. D. Stranks, V. Bharti, J. Gaur, D. Mohanty, S. Chand, H. J. Snaith and N. Robertson, *J. Mater. Chem. A*, 2013, **1**, 6949–6960.
4. H. D. Pham, T. T. Do, J. Kim, C. Charbonneau, S. Manzhos, K. Feron, W. C. Tsoi, J. R. Durrant, S. M. Jain and P. Sonar, *Adv. Energy Mater.*, 2018, **8**, 1703007.
5. H. D. Pham, K. Hayasake, J. Kim, T. T. Do, H. Matsui, S. Manzhos, K. Feron, S. Tokito, T. Watson, W. C. Tsoi, N. Motta, J. R. Durrant, S. M. Jain and P. Sonar, *J. Mater. Chem. C*, 2018, **6**, 3699-3708.
6. X. Yina, L. Guan, J. Yua, D. Zhao, C. Wang, Niraj Shresthab, Y. Han, Q. An, J. Zhou, B. Zhou, Y. Yu, C. R. Grice, R. A. Awni, F. Zhang, J. Wang, R. J. Ellingson, Y. Yan and W. Tang, *Nano Energy*, 2017, **40**, 163-169.
7. T.-T. Bui, M. Ulfa, F. Maschietto, A. Ottochian, M.-P. Nghiêm, I. Ciofini, F. Goubard and T. Pauporté, *Org. Electron.*, 2018, **60**, 22-30.
8. C. Yin, J. Lu, Y. Xu, Y. Yun, K. Wang, J. Li, L. Jiang, J. Sun, A. D. Scully, F. Huang, J. Zhong, J. Wang, Y.-B. Cheng, T. Qin and W. Huang, *Adv. Energy Mater.*, 2018, DOI: 10.1002/aenm.201800538.